

Plasma and BIAS Modeling: Self-Consistent Electrostatic-Particle-In-Cell with low Density Argon Plasma for *TiC*

Jürgen Geiser and Sven Blankenburg

Humboldt-Universität zu Berlin,
Department of Mathematics,
Unter den Linden 6, D-10099 Berlin, Germany
`geiser@mathematik.hu-berlin.de`

Abstract. We motivate our study by simulating the particle transport of a thin film deposition process done by PVD (physical vapor deposition) processes. In this paper we present a new model taken into account a self-consistent electrostatic-particle in cell model with low density Argon plasma.

We propose a collision models for projectile and target collisions in order to compute the mean free path and include the virial coefficients that considered interacting and overlapping gas particles.

The collision model are based of Monte Carlo simulations is discussed for DC sputtering in lower pressure regimes.

We derive an equation for the mean free path for arbitrary interactions (cross sections) which (most important) includes the relative velocity between the projectiles and targets based on physical first principles and extend with higher order Virial terms. In order to simulate transport phenomena within sputtering processes realistically, a spatial and temporal knowledge of the plasma density and electrostatic field configuration is needed. Due to relatively low plasma densities, continuum fluid equations are not applicable. We propose instead a particle-tracking method. Particle-in-cell (PIC) methods allow the study of plasma behavior by computing the trajectories of finite-size particles under the action of an external and self-consistent electric field defined in a grid of points.

Additionally, we apply the electric and magnetic field in the Lorentz forces to obtain a self-consistent electrostatic particle in cell model.

At the target we simulate the deposition rates of the particles *Ti* and *C* based on the Monte Carlo simulations, see idea in [10] and [1].

Keywords: High power pulsed magnetron sputtering, DC sputtering, MAX-phases, mean free path, scattering angle probability distribution, moving targets, Particle-In-Cell-Monte-Carlo-Collisions (PIC-MCC), Maxwell equation, Lorentz force.

AMS subject classifications. 80M31, 60J20, 65N74, 65C05, 65C35, 65C40.

1 Introduction

We motivate our studying on simulating a thin film deposition process that can be done with PVD (physical vapor deposition) processes or sputtering processes.

In the last years, due to the research in producing high temperature films by depositing of low pressure processes have increased. The interest on standard applications to TiN and TiC are immense but recently also deposition with new material classes known as MAX-phases are important. The MAX-phase are nanolayered ternary metal-carbides or -nitrides, where M is a transition metal, A is an A-group element (e.g. Al, Ga, In, Si, etc.) and X is C (carbon) or N (nitride).

We present a model for low temperature and low pressure plasma. The model is derived as a pathway model, see [2], to achieve the deposition rates of the stoichiometry Ti and C .

We taken into account the drift of the ions in the reactor and the less retardation of molecules, which are not treated by the plasma.

The model is discussed as a mass conserved transport problem, modeled with convection-diffusion and reaction equations.

Additionally, we have modeled the electric and magnetic field for the particles, which are controlled by the BIAS voltage of the electrostatic field.

We compare with physical experiments, which measure the different ions and molecule rates in the reactor.

The paper is outlined as follows. In section 2 we present our mathematical model and a possible reduced model for the further approximations. The methods are given in Section 3. Numerical experiments are given in Section 4. In the contents, that are given in Section 5, we summarize our results.

2 Mathematical Model

In the following, we discuss the model of the particle transport in the apparatus between substrate and target. In a next subsection, we describe the electromagnetic field that influences the transport of the ionized particles.

2.1 Collision Model: Mean free path

The mean free path or average distance between collisions for a gas molecule may be estimated from kinetic theory. If one assumes the gas be consisted of hard spheres (non overlapping spheres), then the effective collision area is given by

$$\sigma = \pi (d_1 + d_2)^2 = \pi D^2 \quad (1)$$

In time δt , the area sweep out the volume $V_{interaction}$ and the number of collisions can be estimated from the number of target molecules (n_V) that are in that volume.

$$V_{interaction} = \sigma v \delta t \quad (2)$$

$$\lambda = \frac{|v_{proj}|\delta t}{V_{interaction}n_V} = \frac{|v_{proj}|\delta t}{\pi D^2 v \delta t n_V} = \frac{1}{\pi D^2 n_V} \quad (3)$$

This expression for the mean free path is a good approximation, but it suffers from a significant flaw - it assumes the target objects being at rest, which is of course physically nonsense. By introducing an relative velocity between the gas objects

$$v_{rel} = \sqrt{2}v \quad (4)$$

Whereby the $\sqrt{2}$ results from the molecular speed distribution of a mono atomic ideal gas (Maxwell Boltzmann distribution). We therefore have the expression

$$\lambda = \frac{1}{\sqrt{2}\pi D^2 n_V} \quad (5)$$

The number of molecules per unit volume can be determined from the state equation of the gas

$$pV = (1 + B_1 + B_2 + \dots) RT \quad (6)$$

If one assumes an ideal gas (non interaction and non overlapping gas particles) one can neglect the so called higher Virial coefficients ($B_1 + B_2 + \dots$). Inserting the state equation for an ideal gas into ..., one gets

$$\lambda = \frac{(1) RT}{\sqrt{2}\pi D^2 N_A p} \quad (7)$$

Whereby R is the gas constant and N_A is Avogadro's number. This is an approximation for mean free path for an atom/molecule of an ideal gas. In our problem however, we have to calculate the mean free path of an external particle (projectile) which is not a member of the background gas (ideal gas). This can be done by modifying the average relative velocity between projectile and target. This is done in the next part.

2.2 The Mean Relative Velocity between projectiles and targets

The background gas is assumed to be Maxwell distributed in velocity (this is motivated by the assumption of an ideal gas). Because of the fact that the background particles being a particle ensemble (with statistically distributed velocities) one can just speak of a mean relative velocity $\langle |\mathbf{v}_{rel}| \rangle = \langle |\mathbf{v}_{proj} - \mathbf{v}_{target}| \rangle$, which can be calculated via:

$$\langle |\mathbf{v}_{rel}| \rangle = \int \int \int_V |\mathbf{v}_{proj} - \mathbf{v}_{target}| Z(\mathbf{v}_{target}) d\mathbf{v}_{target} \quad (8)$$

Where Z is the three-dimensional Maxwell distribution given by

$$Z(\mathbf{v}_{target}) = (A/\pi)^{3/2} \frac{1}{2\sqrt{2}} \exp(-A\mathbf{v}_{target}^2) \quad (9)$$

With the abbreviation $A = M_{target}/2k_B T$. A complete derivation of the solution can be found in the appendix. The result is

$$|\mathbf{v}_{rel}| = \frac{\left[\left(s + \frac{1}{2s} \right) \operatorname{erf}(s) + \frac{1}{\sqrt{\pi}} \exp(-s^2) \right]}{3s} \times |\mathbf{v}_{proj}| \quad (10)$$

With $s = a\sqrt{A}$ (scalar) and $a = |v_{proj}|$. We now want to discuss a few special cases.

If the velocity of the projectile is very small $|v_{proj}| \approx 0$, then $s \approx 0$ and therefore the following approximation holds

$$v_{rel} \approx v_{target} \quad (11)$$

Which gives equation number 3 as expected.

If the targets objects are identical the projectile objects (same mass and same mean velocity), then the following limit holds

$$|v_{rel}| \approx 1.41 |v_{target}| \quad (12)$$

Which gives the factor $\sqrt{2} \approx 1.41$ and leads to the mean free path of an element of an mono atomic ideal gas (as expected). However, the general expression for the mean free path of a projectile probing into an ideal gas with pressure P_{gas} and temperature T is given by

$$\lambda_{proj} = \frac{3}{4\pi} \frac{s}{\left[\left(s + \frac{1}{2s} \right) \operatorname{erf}(s) + \frac{1}{\sqrt{\pi}} \exp(-s^2) \right]} \frac{k_B T}{(R_{ion} + R_{target})^2 P_{gas}} \quad (13)$$

There are a few things to say about this expression. First, the main assumption that the background gas (ensemble of target particles) is an ideal gas, is just valid within the high vacuum regime, i.e. small target density. Second, the interaction between the the projectile and target atoms are assumed of hard sphere type, i.e. purely geometric interaction. If the projectile is a free particle between the interactions, its Hamilton function reads

$$H = \frac{p^2}{2M_{proj}} = E \quad (14)$$

In this case one can easily compute $a = |\mathbf{v}_{proj}| = \sqrt{\frac{2E}{M_{proj}}}$. It follows immediately

$$s = a\sqrt{A} = \sqrt{\frac{E}{k_B T}} \sqrt{\frac{M_{target}}{M_{proj}}} \quad (15)$$

In appropriate units (atomic units) the scalar s reads:

$$s = 107.7242 \sqrt{\frac{E[eV]}{T[K]}} \sqrt{\frac{M_{target}}{M_{proj}}} \quad (16)$$

And therefore the mean free path in units of cm is given by:

$$\lambda_{proj}[cm] = \frac{s}{\left[\left(s + \frac{1}{2s} \right) \text{erf}(s) + \frac{1}{\sqrt{\pi}} \exp(-s^2) \right]} \times \frac{3.297\text{cm} \cdot T[K]}{(R_{ion}[pm] + R_{target}[pm])^2 P_{gas}[mbar]} \quad (17)$$

Eklund ([4]) used a formula for the mean free path of ions surrounded by an ideal gas of pressure p_{ar} given by

$$\lambda[cm] = \frac{4.39\text{cm} \cdot T[K]}{\sqrt{\left(1 + \frac{M_{ion}}{M_{target}} \right) (r_{ion}[pm] + r_{target}[pm])^2 p_{target}[mbar]}} \quad (18)$$

The following table shows the mean free path for ions at $E = 3\text{eV}$ and $T = 300\text{K}$ and gas pressure $p = 4 * 10^{-3}$ mbar.

Ion	eqn. 17	eqn. 18
carbon (12)	12.96cm	15.18cm
silicium (28)	7.52cm	7.71cm
titanium (48)	5.03cm	4.55cm

In a sputtering process, the the ions obey a kinetic-energy distribution as well as an angular-distribution at the target. Because of different transport mechanism, the ion looses some extend of their initial kinetic energy. An individual ion within a sputter process can therefore be classified into three groups. First, the **ballistic group**, which is excelled in the way that any member of the ballistic group travels from the target to the substrate in a straight line, because no collisions occur. The **transition group** is characterized by the observation that the path of the ion is not a straight line and therefore the ions of this group undergo some collisions but still retain some of their initial energy. The last group is the **thermalized or diffusive group**, whereby any member of this group is characterized by an complete loss of their initial kinetic energy. The motion of such an ion is therefore described by a random walk. The typical distances between the target and the substrate are of the order of 5 – 15cm. Hence, at low argon pressures we can classify carbon as more or less ballistic, and silicium and titanium as transition or thermalized. One can also see that the formula used by Eklund (2007) ([4]) is quite a good approximation, although it lacks from an energy dependency of the mean free path with respect to the ion energy. There are several attempts to achieve an energy dependency in the mean free path. But most of them are more or less physical consistent. For example, Mahieu et al. (2006) [11] use a formula, whereby the energy dependency is arrived by modifying the naive mean free path by multiplying the naive formula with the ion energy. This is of course unphysical because it implies an infinite mean free path at very high

ion energies (more precise the associate cross section cannot be normalized, i.e. unitarity violation of the cross section). Our mean free path equation is always finite and therefore no violation of unitarity is expected. We hope that our formula for the mean free path will positively accepted within the community and might help to implement a realistic description of the interactions between particles. In figure 1 one can see the results from eqn. 16 and 17 with respect to the ion energy E (kinetic energy) at an argon pressure of $p = 4 \cdot 10^{-3}$ mbar and a constant temperature of $T = 700$ K, whereby the following constants were used.

element	atomic mass [u]	atomic radius [pm]
Ar	39.948	71
C	12.0107	67
Si	28.0855	110
Ti	47.867	150

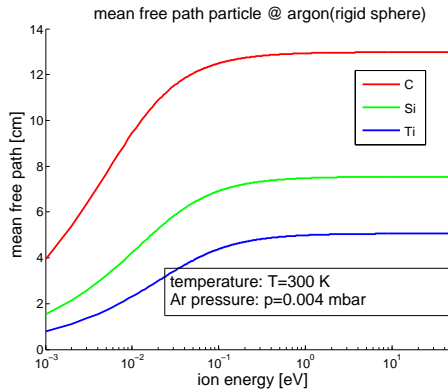


Fig. 1. mean free path of projectiles @ argon targets ($p = 4 \cdot 10^{-3}$ mbar and $T = 300$ K).

2.3 Electro-magnetic Field

For the electro-magnetic field, we have the following assumptions:

Assumptions 1 – *We decouple between ions and electrons*

(electrons behave like perfect fluid, due to lower mass)

– *We apply Monte Carlo Particle-in-Cell simulations for the transport of the particles*

(of the order of 10 mio. particles)

– *We apply optimized iterative solver for the Maxwell equations.*

We deal with the following equations:
The Lorentz force for the particles is given as

$$\mathbf{F} = q \cdot \mathbf{E} + q \cdot \mathbf{v} \times \mathbf{B}, \quad (19)$$

where F is the Lorentz force on each particle, \mathbf{E} the electric field (in volts per meter) and \mathbf{B} the magnetic flux density (in teslas). Further q is the electric charge of the particle (in coulombs) and \mathbf{v} is the instantaneous velocity of the particle (in metres per second).

We denote \times is the vector cross product.

Further we have $\mathbf{B} = \mu\mathbf{H}$, where μ is the magnetic permeability and \mathbf{H} the magnetic field.

Further, we have:

$$\mathbf{E} = -\nabla\Phi, \text{ with } \nabla^2\Phi = -\rho/\epsilon_0 \quad (20)$$

$$\text{and } \nabla \cdot \mathbf{B} = 0 \quad (21)$$

where $\Phi(x, y)$ is the scalar field representing the electric potential at a given point. ρ charge density in space and ϵ_0 the permittivity of free space (electric constant).

Further we denote

$$\nabla \times \mathbf{B} = \mu_0\epsilon_0 \frac{\partial \mathbf{E}}{\partial t} + \mu\mathbf{j} \quad (22)$$

and

$$\nabla \times \mathbf{E} = -\frac{\partial \mathbf{B}}{\partial t} \quad (23)$$

while the ion charge is given in the following equations:

$$\rho = e(Z_i n_i - n_e) = \rho(x, y, t) \quad (24)$$

with Z_i is the charge of ion i and density n ,

The Electrons as fluid is given as

$$n_e = n_0 \exp\left(\frac{\Phi - \Phi_0}{K_B T_e}\right), \quad (25)$$

where K_B is the Boltzmann's constant, n_0 is the mean concentration of charges of the electrons. T_e is the temperatures of the electrons. Further, Φ_0 is the mean charge of the electrons.

For we have the following parameters for the computations of the discretized schemes:

- Debye Length: $\lambda = \sqrt{\epsilon_0 T_e / n_0 e}$
- Thermal velocity of ions: $v_{th} = \sqrt{K_B T_e / M_{ion}}$
- Drift velocity of ions: v_{drift} : was varied between 5000 and 9000 m/s

- Operator discretization via finite difference scheme
(spatial: in units of Debye Length, temporal: $0.1\lambda/v_{drift}$)

We solve the equation of Motion Solver with the Leap Frog method (simplest symplectic integrator).

Further we assume:

- Sputter Particles are Boltzmann distributed with a mean energy of 2 eV
- Angular distribution of sputtered particles is assumed to be Gaussian with mean value of 0 degree and a variance of 10 degrees.

3 Monte Carlo simulations

In the following we apply the Monte Carlo simulation, that is based on the collision model for the DC sputtering and the Coloumb model for the HIPIMS sputtering, see [7].

3.1 Angular distribution

The angular distribution of out-coming particles from the sputter material is modeled by a sine distribution, i.e. the relative amount of particles leaving the sputter material perpendicular to its surface ($\theta_0 = 90$) is 1. Differences in the angular distribution between the different species are not modeled but can not experimentally excluded.

3.2 Ionization rates and ion energy distribution

The ionization rate of sputtered particles are very low, and thus no influence on the particle distribution is assumed. But in contrast, the particle's energy seems to be of high importance. Unfortunately, until now no energy distribution for our compound target (*TiC*) is available. In figure 2 one can see the ion energy distribution, which is modeled with reference to a Ti-target. One can see that most of the ions are at energies close to 3eV. In order to simulate the ion transport it is necessary to calculate the velocity of the ions. With

$$E = H = \frac{p^2}{2M} = \frac{1}{2}Mv^2$$

it follows that

$$v = \sqrt{\frac{2E}{M}} \quad (26)$$

The energy of the ions is given in units of electron volts (eV) and the mass of the ions is given in atomic units (u). Therefore one can compute the velocity in units of cm per second by using

$$v = \sqrt{\frac{2E[eV]}{m[u]}} \cdot 9.824 \cdot 10^5 = v[cm/s] \quad (27)$$

In two spatial dimensions, one has two velocity components. ϕ_0 is the direction angle of the ion (see angular distribution of the ions) the velocity components can be calculated by

$$v_x = v \cdot \cos(\phi_0) \quad (28)$$

$$v_y = v \cdot \sin(\phi_0) \quad (29)$$

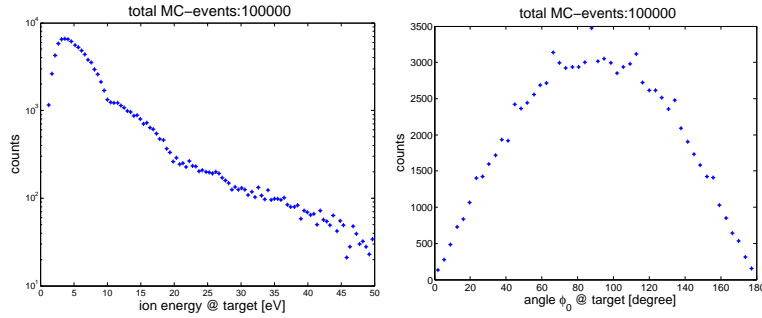


Fig. 2. energy distribution and angular distribution of the sputtered species at the target.

Now, we want to apply our two interaction models to DC and high power pulsed sputtering for *TiC*. In general if several independent interaction mechanism can occur, the mean free path is not an additive quantity, but in contrast the total cross section is an additive quantity. In order to reduce the computational effort, we decided to use an event-driven Monte Carlo method in contrast to the usually used time-driven Monte Carlo method. It is therefore necessary to determine, when the next interaction will occur. If the velocity (v) and the mean free path (λ) of the particle is known, one can compute the collision frequency τ by using

$$\tau = \frac{v}{\lambda} = \frac{\sqrt{v_x^2 + v_y^2}}{\lambda} \quad (30)$$

With the help of the collision frequency one is able to compute the time interval until the interaction occurs

$$\delta t = -\frac{\log(r)}{\tau} \quad (31)$$

Whereby r is a random number from a uniform distribution between zero and one. Instead of simulating the trajectory of all particles in a Monte Carlo run with a fixed time step, one can use the above mentioned formula to adjust the time step. the strategy is as follows, one calculates the time interval δt for every particle (except the background particles) within a Monte Carlo run (trial), and finds the minimum value. The particle related to the minimum value of

δt will first undergo an interaction. The Monte Carlo time step is set to this minimum value (event driven MC). After the time step, the specific particle will undergo the interaction, and all other particles are just move along they're specific trajectory. i.e. in the absence of any external forces the trajectory is just a straight line (this is motivated by the fact the even if external fields are set up, inside the plasma the particles will behave as if they were free, due to the electric conductance of the plasma). If an interaction with the background gas (argon) occurs, we assume a uniform impact parameter distribution in the center-of-mass-system (CMS) between the ion and the background gas. We first describe the simulations of DC sputtering thereafter the simulations concerning high power pulsed magnetron sputtering. The several interaction processes can be put into an abstract interaction model (Pathway model, see [2]) that binds the interaction parameter together. A schematic drawing can be seen in fig. 3.

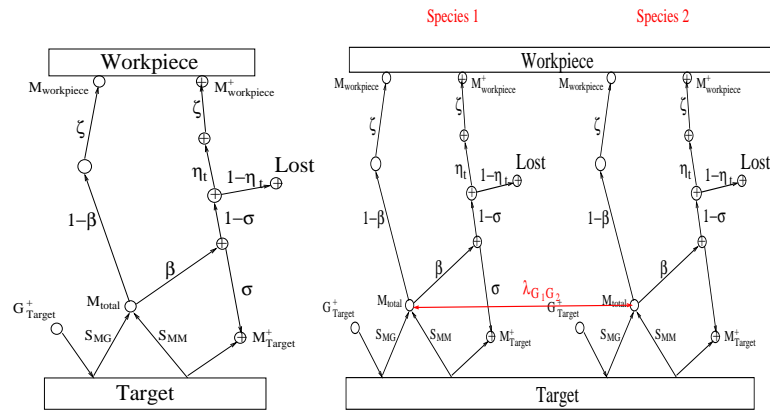


Fig. 3. **left:** Single (Christie 2005) and **right:** Multiple (2 species) Pathway model (Geiser 2008).

4 Numerical Experiments

In the following, we discuss the numerical experiments, based on the influence of the particle flow via the BIAS voltage.

Here the idea is to control the deposition rate with the BIAS voltage.

4.1 First Numerical Experiment: Delicate Geometry

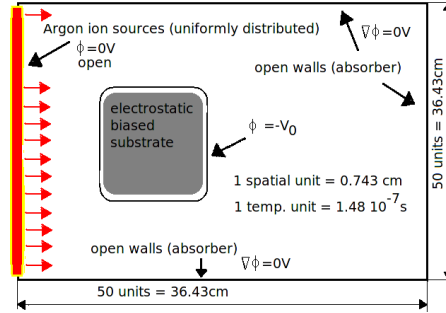
In the first experiment we study the influence of a delicate geometry to the DC-sputter process.

We apply an efficient Particle-in-Cell Monte Carlo Simulation of an argon plasma in C++ (Multiprocessor implementation via OpenMP). The simulations

of arbitrary substrate geometries are performed, ion sources and electrostatic boundary conditions are possible to implement.

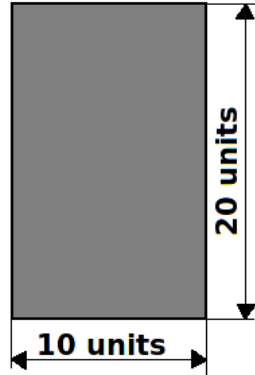
We compute the spatial ion distribution between target and substrate (electrostatic biased) as well as spatial self-consistent electrostatic field configuration at equilibrium time (macroscopic time scale).

Next, we have the general setup in the reactor:

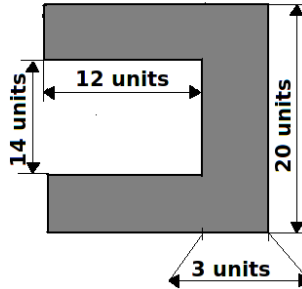


For the computations we studied the following objects as target:

Object A&B



Object C



The parameters for the electric-field equations are given as:

Quantity	Value
Electron Density n_0	$10^{12} m^{-3}$
Electron Temperature T_e	$1eV$

The experiment A, we choose the $U_{bias} = -100V$ and $v_{drift} = 5000m/s$. The results are given in Figure 4.

The experiment B, we choose the $U_{bias} = -50V$ and $v_{drift} = 5000m/s$. The results are given in Figure 5.

The experiment C, we choose the $U_{bias} = -150V$ and $v_{drift} = 5000m/s$.

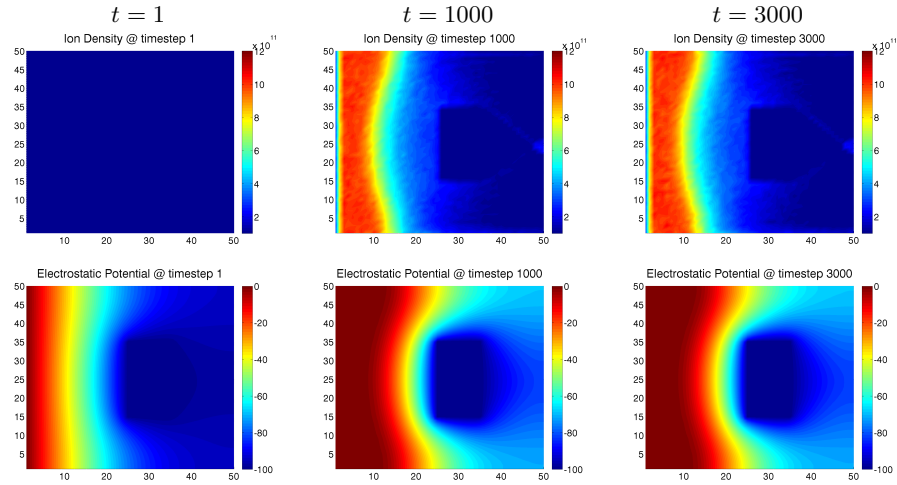
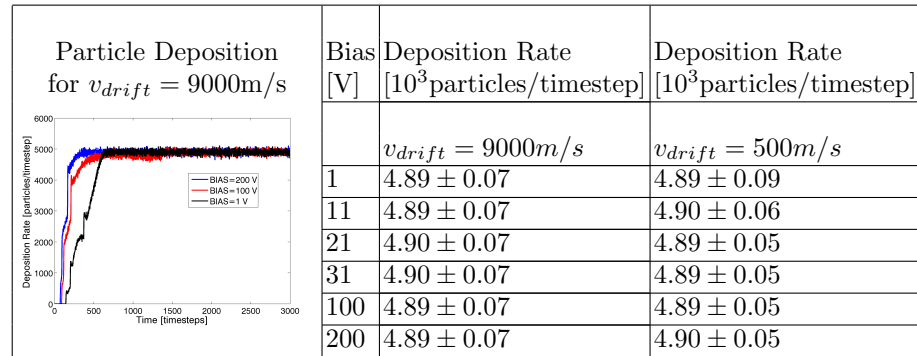


Fig. 4. Target experiment with $U_{bias} = -100V$ and $v_{drift} = 5000m/s$

The results are given in Figure 6.

A Phenomenological Study: Deposition-Rate (Object A)

We measured the equilibrium deposition rate with respect to the BIAS voltage at the substrate. In order to estimate the deposition rate we used the first 1500 time steps for coming to equilibrium and the following 1500 time steps for our measurement.



Remark 1. In the experiments, we show the influence of the deposition rates at macroscopic time scales seems with respect to the underlying BIAS voltage.

In this experiments, we neglect the magnetic field in the Lorentz forces and it seems that the deposition rates are independent of the BIAS voltage.

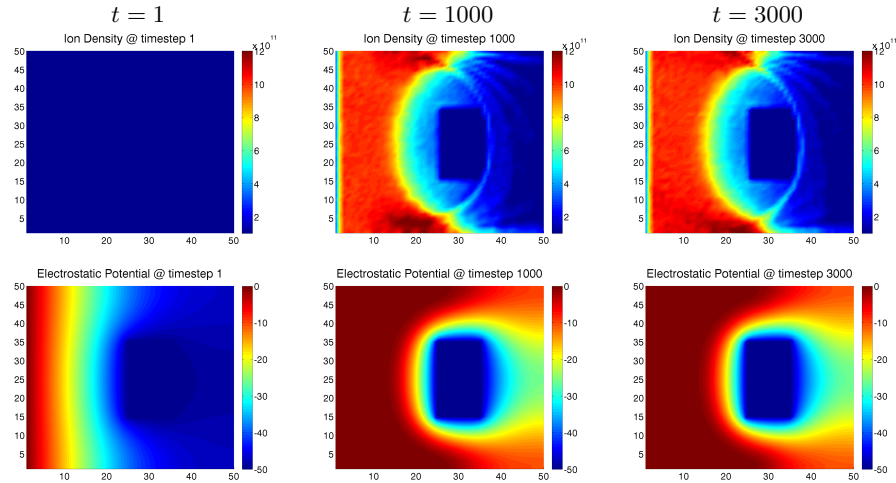


Fig. 5. Target experiment with $U_{bias} = -50V, v_{drift} = 5000m/s$

4.2 Second Numerical Experiment: Delicate Geometry (concerning the magnetic field in the Lorentz force on each particle)

In the second experiments, we taken into account the full Lorentz force on each particle.

We simulate the paths of the sputtered atoms Ti and C and obtain at least a clue of the stoichiometric decomposition at the substrate.

We apply the full model (full Lorentz force) of an interaction between the sputtered particles and the background gas (Ar).

Due to relatively low plasma densities we consider our particle-in-cell (PIC) methods and study the plasma behavior by computing the trajectories of finite-size particles under the action of an external and self-consistent electric field defined in a grid (200×200) of points. For the shown results, we use a computer cluster of 4×8 Intel(R) Xeon(R) CPU X5472 @ 3.00GHz and a total memory of 64 GByte (due to large electrostatic and magnetostatic grids).

We solve the ion-electrostatic field feedback mechanism (self-regulating dynamic mechanism) and complex fields due to biased complex substrate geometries (mixed electrostatic boundary conditions) with the discussed methods..

By decoupling the ions and electrons (electrons behave like perfect fluid, due to lower mass) we could save computational time.

The Monte Carlo Particle-in-Cell simulations are only done for the transport of the ions, we use the order of 10 mio. particles.

Based on the electric field, we have a transition from event-related MC to time-related MC (while computing the electrical influence to the ions).

Here, we study the influence of a delicate geometry with respect to the Lorentz forces of a DC-sputter process.

We have the general setup in the reactor:

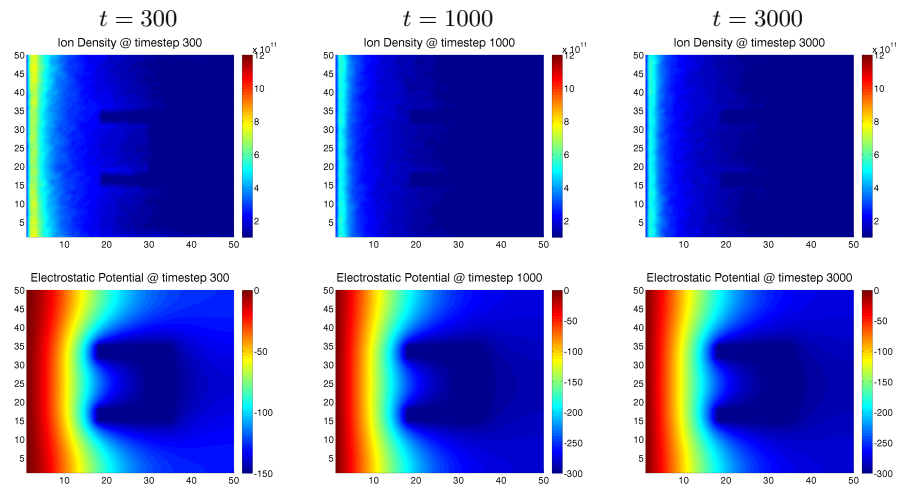
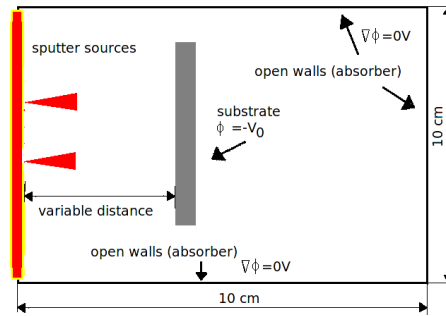


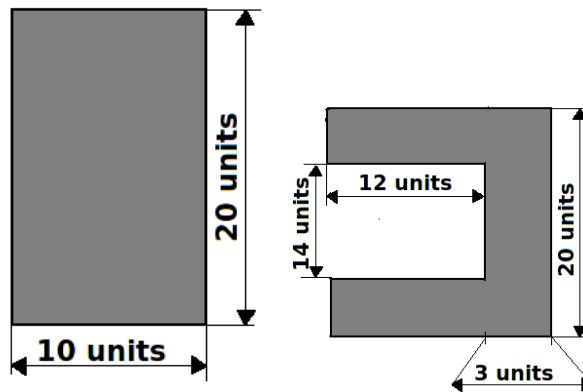
Fig. 6. Target experiment with $U_{bias} = -150V$, $v_{drift} = 5000m/s$



For the computations we studied the following objects as target:

Object A&B

Object C



The parameters for the electric-field equations are given as:

Quantity	Value
Electron Density n_0	$10^{12} m^{-3}$
Electron Temperature T_e	$1eV$

The experiment A, we choose the Ar-Density= $4 \cdot 10^3$ mbar, $(Ti, C) = (0.7, 0.1)$.

The results are given in Figure 7.

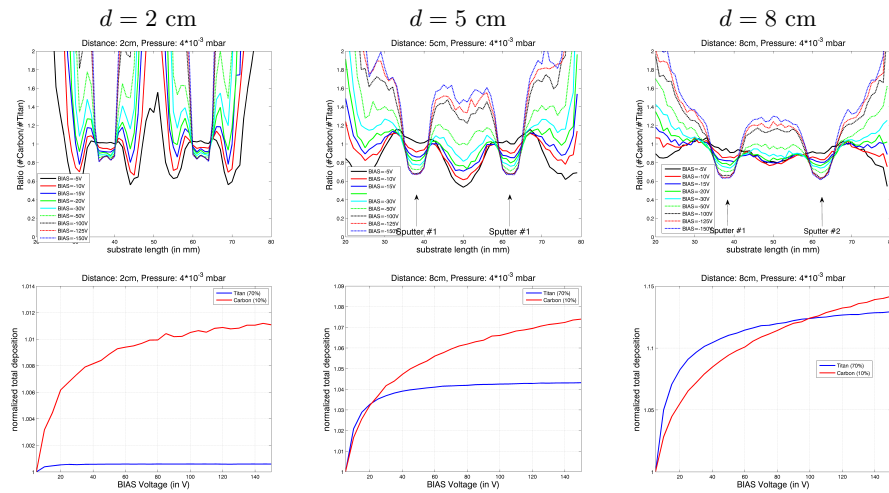


Fig. 7. Target experiment with Ar-Density= $4 \cdot 10^3$ mbar, $(Ti, C) = (0.7, 0.1)$.

The experiment B, we choose the Ar-Density= $4 \cdot 10^3$ mbar, $(Ti, C) = (0.5, 0.05)$.

The results are given in Figure 8.

The experiment C, we choose a realistic test geometry by cooperation partner M. Balzer (FEM, Schwäbisch Gmünd, Germany) with the parameters: Ar-Density= $4 \cdot 10^3$ mbar, $(Ti, C) = (0.5, 0.05)$, Distance= 60 mm.

The results are given in Figure 9.

The experiment D, we test the influence of a non planar substrates with the parameters: Ar-Density= $4 \cdot 10^3$ mbar and different distances.

The results are given in Figure 10.

Remark 2. In the experiments, we show the influence of the deposition rates at macroscopic time scales seems with respect to the underlying BIAS voltage. For the full model (with magnetic field in the Lorentz force), we obtain a dependency of the BIAS voltage to the deposition rate. In the arbitrary substrate geometries, we obtain the best stoichiometric composition at BIAS voltage of about -30

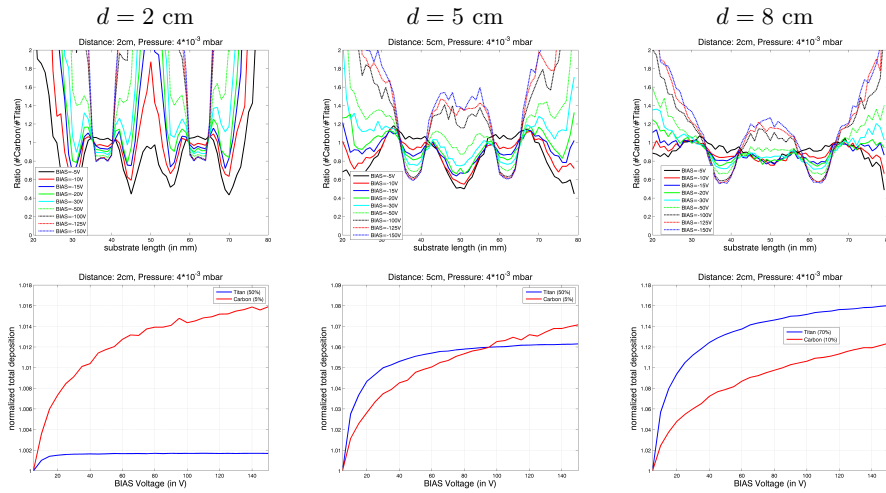


Fig. 8. Target experiment with Ar-Density= $4 \cdot 10^3$ mbar, $(Ti, C) = (0.5, 0.05)$.

V and moderate Target-Substrate-Distances around 8 cm and a moderate Ar-Density of about $4 \cdot 10^{-3}$ mbar. Further, we found out, that an important quantity for non planar substrates is the ratio of the width and the depth of an inlet. So it makes sense to have at least small inlets to obtain a homogeneous deposition on the target.

5 Conclusions and Discussions

We present a novel model to consider DC and HIPIMS sputter processes in real gas regimes. We extend the underlying transport model by a Maxwell equation to model the electro-magnetic field. The electrostatic field based on an additional BIAS voltage allows control the ionized particles. We can improve the deposition rate in delicate geometrical zones. Mathematically we solve coupled transport and Maxwell equations, while we apply the optimal solvers for each separate equations. Numerical results are presented and compared to real life applications, that allows to estimate an optimal BIAS voltage about $-5 [V]$ to $-30 [V]$.

References

1. D.J. Christie. *Particle-In-Cell with Monte Carlo Collision Gun Code Simulations of a Surface-Conversion H^- Ion Source*. Communications in Computational Physics, Vol. 4, No. 3, 659-674, 2008.
2. D.J. Christie. *Target material pathways model for high power pulsed magnetron sputtering*. J.Vac.Sci. Technology, 23:2, 330-335, 2005.
3. P. Eklund, M. Beckers, J. Frodelius, H. Högberg, and L. Hultman. *Magnetron sputtering of Ti_3SiC_2 tin films from a compound target*. JVST A, 25(5):1381-1388, 2007.

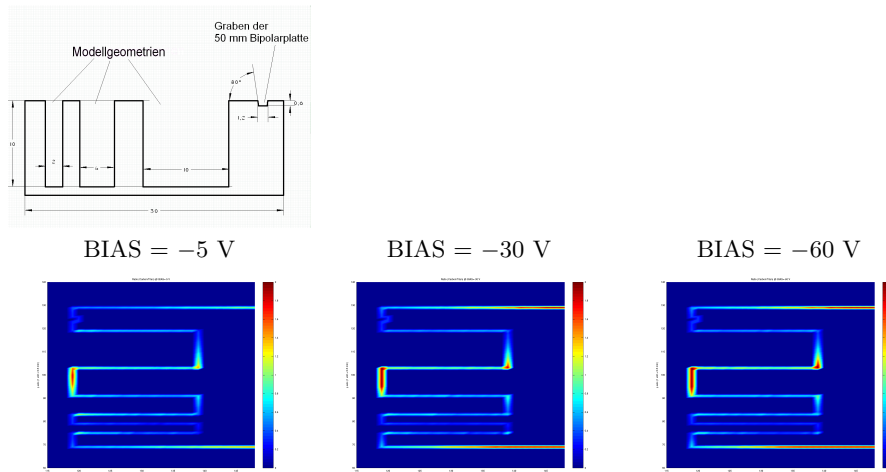


Fig. 9. Target experiment (realistic test geometry) with Ar-Density= $4 \cdot 10^3$ mbar, $(Ti, C) = (0.5, 0.05)$ and Distance= 60 mm.

4. P. Eklund. *Multifunctional nanostructured Ti-Si-C thin films*. Linköping studies in science and technology, Dissertation No. 1087, 2007
5. E. Everhart, G. Stone, R. J. Carbone. *Classical Calculation of Differential cross section for Scattering from a Coulomb Potential with Exponential Screening*. Physical Review Volume 99, Number 4:1287-1290, 1955.
6. J. Geiser, R. Roehle. *Modeling and Simulation for Physical Vapor Deposition: Multiscale Model*. Journal of Convergence Information Technology, Korea, published, November 2008.
7. J. Geiser, S. Blankenburg. *Monte Carlo simulations concerning elastic scattering with application to DC and high power pulsed magnetron sputtering for Ti₃SiC₂*. Preprint 2009-20, Humboldt University of Berlin, Department of Mathematics, Germany, 2009.
8. H. Goldstein. *Classical Mechanics*. Addison-Wesley Series in Physics, Second edition (1980).
9. H.H. Lee. *Fundamentals of Microelectronics Processing* McGraw-Hill, New York, 1990.
10. S. Longo, M. Capitelli and K. Hassouni. *The Coupling of PIC/MCC Models of Discharge Plasmas with Vibrational and Electronic Kinetics*. J. Phys. IV France 7, Colloque C4, 271-281, 1997.
11. S. Mahiheu, G. Buyle, D. Depla, S. Heirwegh, P. Ghekiere, R. De Gryse. *Monte Carlo simulation of the transport of atoms in DC magnetron sputtering*. Nuclear Instruments and Methods in Physics Research B 243:313-319, 2006.
12. S. Middleman and A.K. Hochberg. *Process Engineering Analysis in Semiconductor Device Fabrication* McGraw-Hill, New York, 1993.
13. M. Ohring. *Materials Science of Thin Films*. Academic Press, San Diego, New York, Boston, London, Second edition, 2002.
14. P.J. Roache. *A flux-based modified method of characteristics*. Int. J. Numer. Methods Fluids, 12:1259-1275, 1992.

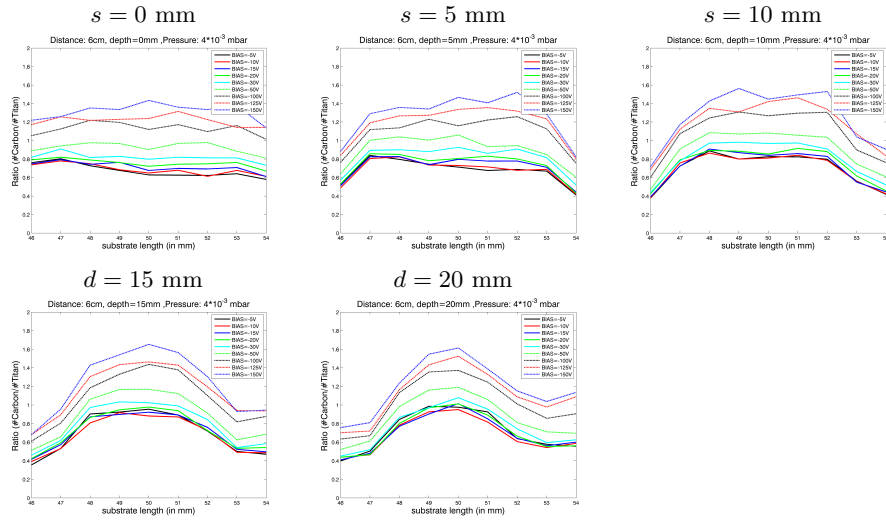


Fig. 10. Target experiment (realistic non-planar substrates) with Ar-Density= $4 \cdot 10^3$ mbar and different distances.

15. A. Russek. *Effect of Target Gas Temperature on the Scattering cross section*. Phys. Rev. 120, 1536 - 1542 (1960).
16. T.K. Senega and R.P. Brinkmann. *A multi-component transport model for non-equilibrium low-temperature low-pressure plasmas*. J. Phys. D: Appl.Phys., 39, 1606–1618, 2006.